

12-18-2011

Septotemporal Variation in Theta Rhythm Dynamics: Effects of Speed and Habituation

James Hinman

University of Connecticut, james.hinman@uconn.edu

Recommended Citation

Hinman, James, "Septotemporal Variation in Theta Rhythm Dynamics: Effects of Speed and Habituation" (2011). *Master's Theses*. 209.
https://opencommons.uconn.edu/gs_theses/209

This work is brought to you for free and open access by the University of Connecticut Graduate School at OpenCommons@UConn. It has been accepted for inclusion in Master's Theses by an authorized administrator of OpenCommons@UConn. For more information, please contact opencommons@uconn.edu.

**Septotemporal Variation in Theta Rhythm Dynamics: Effects of
Speed and Habituation.**

James Richard Hinman

B.A., Psychology, University of Connecticut, 2006

A Thesis

Submitted in Partial Fulfillment of the

Requirements for the Degree of

Master of Arts

at the

University of Connecticut

2010

APPROVAL PAGE

MASTER OF ARTS THESIS

Septotemporal Variation in Theta Rhythm Dynamics: Effects of Speed and Habituation.

Presented by

James Richard Hinman, B.A.

Major
Advisor

James J. Chrobak, Ph. D.

Associate
Advisor

Monty A. Escabí, Ph. D.

Associate
Advisor

Heather L. Read, Ph. D.

TABLE OF CONTENTS

	<u>PAGE</u>
CHAPTER 1: Introduction	
Cell assembly coordination by theta and gamma oscillations	1
Theta and gamma generation	3
Anatomical organization of the hippocampal formation	5
Physiological differentiation along the Septotemporal Axis	10
CHAPTER 2: Septotemporal variation in theta rhythm dynamics	
Introduction	11
Methods	17
Results	24
Discussion	37
CHAPTER 3: Discussion	45
REFERENCES	55

LIST OF FIGURES

		<u>PAGE</u>
FIGURE 1	Circuitry involved in theta current generation	7
FIGURE 2	Electrode positions and running behavior	23
FIGURE 3	Theta power across the septotemporal axis	25
FIGURE 4	Single animal example of speed modulation of theta power throughout the hippocampal formation	26
FIGURE 5	Variation in speed modulation of theta power across the septotemporal axis	27
FIGURE 6	Variation in theta power habituation across the septotemporal axis	30
FIGURE 7	Speed modulation of theta coherence throughout the hippocampal formation	34
FIGURE 8	Delayed match to place T-maze task	52

Chapter 1

Introduction

Cell assembly coordination by theta and gamma oscillations

Theta and gamma oscillations are theorized to provide a clocking mechanism that can bring physically separated groups of cells together in time, potentially allowing for the integration or segregation of distant cell assemblies. Since the slower theta rhythm is generated by the rhythmic excitation of cells throughout the hippocampus, it can be thought of as providing a time window for the activation of cells across a large area. The faster gamma rhythm coordinates smaller groups of cells, or cell assemblies, and these smaller packets of information are grouped or synchronized by the slower theta rhythm. Thus local cell assemblies throughout the hippocampus can be activated during individual bouts of gamma occurring at a particular phase of theta. In such a manner, cell assemblies that are separated by a vast and physically insurmountable distance (for a neuron) can come together in time to represent information in a distributed manner.

Such coordination of cell assemblies across the septotemporal axis of the hippocampus by the theta rhythm requires that the theta signals generated locally at all sites along the septotemporal axis be coherent. This is an assumption that is typically made (Buzsaki, 2002) and as a result studies are often conducted using a theta signal recorded from a single site as a reference

for phase locking activity in a variety of other brain regions (Chrobak and Buzsaki, 1994; Bragin et al., 1995; Hyman et al., 2005; Maurer et al., 2005; Jones and Wilson, 2005). Until recently investigations into the coherence of theta across the septotemporal axis had typically been limited to about 2 – 3 mm (Bullock et al., 1990; Bragin et al., 1995), yet the entire length of the dentate gyrus in the rat is about 10 – 12 mm. Bullock et al. (1990) showed that theta coherence decreased from about 1.0, with electrodes spaced about 0.2 mm apart, to about 0.7 when electrodes were positioned 2 mm apart along the septotemporal axis of CA1. Recently investigations have shown that theta coherence decreases as a function of the distance between sites spanning the majority of the septotemporal axis (Sabolek et al., 2009, Royer et al., 2010), with theta coherence values dropping below 0.3 at distances > 5.0 mm. Thus the theta signals locally generated at different sites along the septotemporal axis become increasingly different as the distance between the sites increases.

While it is the general case that theta coherence decreases as a function of distance along the septotemporal axis, there is variability in the degree of this coherence over time. Theta coherence between two distant electrodes can rise and fall, potentially allowing for the integration or segregation of cell assemblies at those sites. In addition to variability in theta coherence, theta power at an individual site varies widely over time and it is explaining the source of variability in a number of spectral indices of theta that is the goal of this work.

Theta and gamma generation

The generation of theta and gamma field potential oscillations has been extensively studied in septal HPC, as well as in EC, and it has been shown that the laminar organization of cell bodies, parallel arrangement of dendrites and the specificity of excitatory inputs in the hippocampus provides an ideal organization for the generation of large amplitude local field potential (LFP) oscillations. Theta (6-12 Hz) and gamma (40-100 Hz) LFP oscillations are generated by the summation of synchronous excitatory and inhibitory potentials impinging upon the laminarly structured architecture of the hippocampal formation (HF; EC, DG, CA3, CA1, subiculum), as well as intrinsic membrane oscillations of principle cells (Green & Arduini, 1954; Petsche et al., 1962; Leung, 1984; Bland, 1986; Bragin et al., 1995; Vinogradova, 1995; Vertes & Kocsis, 1997; Buzsaki, 2002; Montgomery et al., 2009).

Several key circuit elements contribute to theta and gamma current generation (eg, amplitude of LFPs) and synchrony (eg, coherence across sites) including minimally: 1) excitatory entorhinal cortical inputs from layer II – III neurons (Alonso and Garcia-Austt, 1987; Chrobak and Buzsaki, 1998); 2) excitatory (glutamatergic) hippocampal neurons (dentate granule cells, hilar mossy cells, CA3 and CA1 pyramidal neurons); 3) networks of categorically distinct GABAergic neurons (eg, basket cells, chandelier cells, subclasses of dendritic-targeting cells; Ylinen et al., 1995; Konopacki et al., 1992; Hajos et al., 2004); 4) medial septal cholinergic inputs (Brazhnik and Fox, 1999); 5) medial

septal GABAergic neurons that selectively target specific sub-populations of hippocampal GABAergic neurons (Freund and Antal, 1988; Borhegyi et al., 2004, Hangya et al., 2009); 6) GABAergic hippocampo-septal neurons that feedback to the medial septal GABAergic neurons (Toth et al., 1993; Manseau et al., 2008); 7) excitatory input from the supramammillary nucleus to both HPC and the medial septum and 8) several subcortical neuromodulatory inputs (eg, serotonergic, noradrenergic, histaminergic; see Vertes and Kocsis, 1997 for review). While the summation of all of these elements yields the highly regular theta and gamma oscillations observed in the field potential, slight variations in any one of these inputs can result in changes in the power (amplitude) at an individual site or the synchrony (coherence) between sites. Since each of these rhythms is generated relatively independently at sites throughout the HF and there are prominent differences in the distribution of many of the afferents involved in theta generation along the septotemporal axis (see below), it should not be surprising to see systematic, yet independent, behavioral correlates of spectral indices of theta along the septotemporal axis.

While theta and gamma are generated by different mechanisms, their generation tends to covary with each other. Since each theta generating excitatory pathway into and within the hippocampus contacts a unique population of interneurons (Freund and Buzsaki, 1996), the theta rhythmic inputs into each hippocampal subregion modulate both principle cells and their corresponding, categorically distinct GABAergic interneurons. The excitatory potentials that generate theta also rhythmically excite GABAergic interneurons at theta

frequency, which results in the interneurons discharging action potentials during a particular phase of theta. GABAergic interneurons in the HPC have been shown to discharge at gamma frequency (eg, basket cells) and thus are widely thought to be the primary generators of gamma oscillations in the field potential. So even though theta and gamma are generated through different mechanisms, gamma power has been shown to covary with theta power, as well as be phase modulated by the slower theta oscillation in the hilus of the DG (Bragin et al., 1995), as well as in EC (Chrobak and Buzsaki, 1998) of the rat.

The coupling of these two rhythms has been suggested to be computationally very powerful (Lisman and Idiart, 1995). The theta phase modulation of gamma power has been demonstrated in the neocortex and hippocampus of humans (Canolty et al., 2006; Axmacher et al., 2010) and that not only was gamma power modulated by theta phase, but that this relationship varied as a function of task demand. Canolty et al. (2006) showed that the cortical sites showing significant theta phase modulation of gamma power vary according to what task the subject was performing, while Axmacher et al. (2010) showed a systematic variation in the theta modulation of gamma as a function of increasing the load in a working memory task.

Anatomical organization of the hippocampal formation

The variability in the power and coherence of LFP signals independently generated at different sites along the septotemporal axis likely arises due to differential changes in firing of the various afferents involved in theta and gamma

generation and thus an understanding of the underlying anatomy is critical for proper interpretation of LFP data. The hippocampal formation has been described anatomically in great detail previously (Steward and Scoville, 1976; Swanson & Cowan, 1977; Amaral & Witter, 1995; Amaral and Lavenex, 2007), but, briefly, the hippocampal formation consists of the EC, DG, CA3, CA2, CA1, subiculum, presubiculum and parasubiculum. The EC is a six layer cortical structure that provides the primary information bearing cortical input to the HPC via the superficial layers (II & III) and is also the primary cortical recipient of HPC output, which terminates in the deep layers (V & VI). EC layer II stellate cell projections terminate on the dendrites of granule cells in the molecular layer of DG and on the distal apical dendrites of pyramidal cells in stratum lacunosum-moleculare of CA3. EC layer III pyramidal cells project to the distal apical dendrites of pyramidal cells in stratum lacunosum-moleculare of CA1 and the molecular layer of the subiculum. Pyramidal cells of CA1 and the subiculum then send return projections to layers V and VI of EC. While the layer of origin in EC determines the subregional termination within the transverse axis of the HPC, the level of the septotemporal axis that the EC projections terminate in is dependent upon the areal origin within the EC.

The EC is organized into three segregate bands of cells (lateral, intermediate and medial) that are oriented orthogonally to the cytoarchitectonically defined medial and lateral entorhinal areas (MEA & LEA; Dolorfo & Amaral, 1998a; see also Chrobak & Amaral, 2007). Neurons in each of the bands obey two organizing principles regarding their projections: 1) they

project unilaterally to segregate septotemporal extents of the HPC, such that the lateral band projects to the septal 50% of HPC, the intermediate band projects to the next ~25% and the medial band projects to the temporal ~25% and 2) their intrinsic projections remain restricted within each of the segregate band of neurons. As the cells of EC are one of the primary sources of current generation for theta, the fact that segregate groups of cells are projecting to different

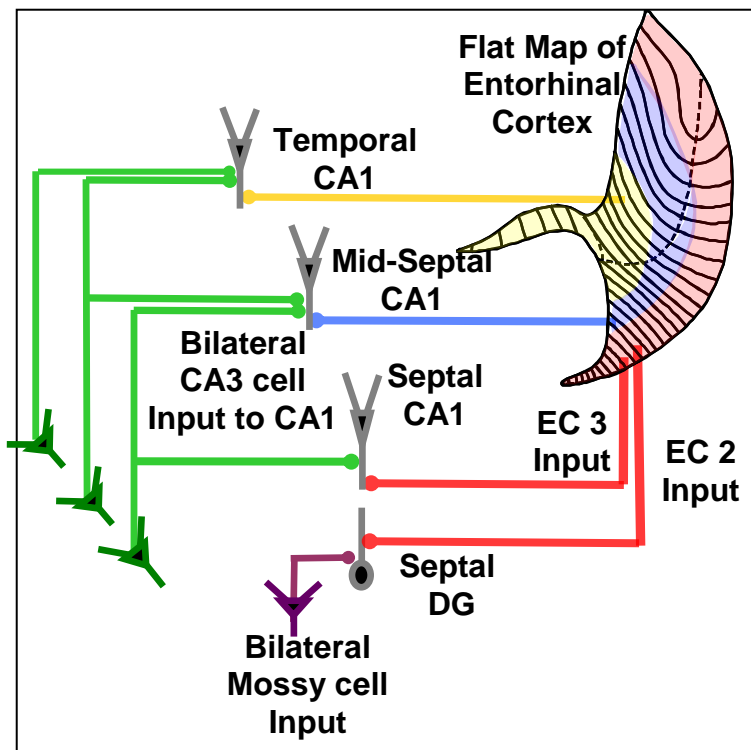


Figure 1. Segregate bands of EC cells project to distinct levels of the septotemporal axis of DG and CA1. In addition to projections to the hippocampus, cells located in each of the EC bands (lateral in red, intermediate in blue and medial in yellow) also have intra-entorhinal projections that remain restricted to the band of origin. Within the hippocampus CA3 pyramidal cells and DG mossy cells project extensively along the septotemporal axis, as well as bilaterally.

septotemporal levels of HPC and that these groups of cells are not interconnected suggests that the EC may be a source of potential differences in theta across the septotemporal axis.

Within the HPC, the principle cells of the various subfields project in a unidirectional manner with DG granule cells projecting to CA3 pyramidal cells, CA3 cells projecting to CA1 pyramidal cells and CA1 cells projecting to subicular

pyramidal cells. CA1 and subicular pyramidal cells are the source of HPC output back to EC with terminations in the layers V-VI. Each of these groups of HPC cells has been shown to generate action potentials phase locked to theta, with CA3 pyramidal cells possessing the capability to generate theta independently of the EC (Bragin et al., 1995). In contrast to the EC projections to HPC that are a potential source of differences in theta across the septotemporal axis, excitatory hilar mossy cells and CA3 pyramidal cells both project extensively along the septotemporal axis thus providing a potential means for synchronizing theta along this dimension.

Another potential source of differences along the septotemporal axis may arise from septohippocampal projections. The medial septum (MS) sends cholinergic and GABAergic projections to the HPC that are organized in a topographic manner. Cells located anteriorly and laterally in MS project to temporal HPC, while cells located more posteriorly and medially project to septal HPC. The cholinergic input from the MS provides a diffuse distribution throughout all subfields of HPC, thus providing a general depolarizing effect on all HPC cells. In contrast, the GABAergic projections to HPC preferentially synapse on HPC perisomatic basket cells. Since MS cells spike in a phase locked manner to theta, the septohippocampal GABAergic projection provides theta rhythmic inhibition to HPC interneurons that are in a powerful position to control HPC principle cells spiking. With different cells in MS projecting to different septotemporal levels of HPC and the fact that the MS is believed to

powerfully control the amplitude of theta, the MS is a well suited candidate for synchronizing or differentiating theta across the septotemporal axis.

At least three glutamatergic inputs to HPC display a graded distribution along the septotemporal axis. First, the supramammillary nucleus preferentially targets the DG with few projections terminating in CA1 (Vertes et al., 1992). Along the septotemporal axis the supramammillary terminations show a graded distribution with a greater density of terminals in septal HPC than in temporal HPC (Vertes et al., 1992). Supramammillary neurons are known to fire trains of action potentials at theta frequency and, in addition to providing input to HPC, supramammillary neurons also innervate the MS where their theta rhythmic firing provides a depolarizing effect that likely increases rhythmicity within the population. Thus the supramammillary nucleus is a key subcortical component of theta generation. Second, the nucleus reuniens is the sole source of thalamic input to HF. Afferents from nucleus reuniens do not reach the septal portion of HPC and thus are only present from approximately midseptotemporal to temporal levels of the septotemporal axis (reference). In addition to showing a septotemporal gradient, nucleus reuniens projections selectively synapse in stratum lacunosum-moleculare of CA1 and the molecular layer of the subiculum where the afferents from EC terminate. Third, input from the amygdala terminates at even more temporally restricted levels of HPC than the nucleus reuniens input (Pikkarainen et al., 1999). These differences in glutamatergic input along the septotemporal axis are not only a potential source of differences in the

theta generated in septal versus temporal levels of the HPC, but also suggest differences in the information processed at the different poles of the HPC.

The last major difference in afferent input across the septotemporal axis involves the distribution of various neuromodulators. Noradrenergic input from the locus coeruleus (LC) shows both a specific laminar distribution within the transverse axis, as well as a graded distribution along the septotemporal axis. LC neurons synapse densely in the hilar region of DG, as well as selectively in stratum lucidum of CA3 and stratum locunosum-moleculare of both CA3 and CA1. Along the septotemporal axis, LC afferents to HPC display a graded increase from septal to temporal levels while still following the transverse distribution just described. Serotonergic input from the raphe nucleus, which terminates primarily in an immediately subgranular aspect of the hilus and stratum locunosum-moleculare of CA1, follows a similar septotemporal gradient as the noradrenergic input. Serotonergic input increases with increasing distance from the septal pole. Lastly, histamine immunoreactive fibers also increase from septal to temporal levels of HPC (Panula et al., 1989). (Loy et al., 1980; Haring and Davis, 1985; Oleskevish and Descarries, 1990; Bjarkam et al., 2003 Gage and Thompson, 1980; Amaral and Kurz, 1985; see also Thompson et al, 2008 for an excellent review).

Physiological differentiation along the Septotemporal Axis

Despite the septotemporal variation in anatomical inputs, physiological investigations in the HPC has primarily been restricted to septal HPC and the

conclusions drawn from septal HPC physiology have typically been tacitly attributed to the entire length of the HPC. Pyramidal cells in septal CA1 have long been known to have spatially restricted receptive fields in a given environment (O'Keefe and Dostrovsky, 1971) and thus have been termed place cells. The population of septal CA1 place cells is believed to form the basis of a cognitive map of an environment and even a limited number (~15-20) of place cells can be used to estimate a rats location in an environment to within a few centimeters (Wilson and McNaughton, 1993). The overwhelming majority of place cells recordings have focused on septal HPC, with only a few published reports venturing to record at midseptotemporal or temporal regions of HPC (Jung et al., 1994; Maurer et al., 2005; Kjelstrup et al., 2008; Royer et al., 2010). The few reports of place cell recordings along the septotemporal axis have shown that the size of a given cells place field increases from septal to temporal levels of CA1 (Jung et al., 1994; Maurer et al., 2005). Recordings from CA3 pyramidal cells at different septotemporal levels have demonstrated a similar pattern, with septal CA3 place cells having receptive fields of about one meter in length along a linear track and temporal CA3 place cells having place fields about 5-6 meters in length when rats traverse an eighteen meter long linear track (Kjelstrup et al., 2008). Thus there is spatial information present in the activity of temporal CA3 place cells, but the spatial scale has increased in a linear fashion from septal to temporal regions. Recently another report verified this increase in spatial scale in temporal CA3 and additionally suggested that non-spatial information was coded by temporal CA3 pyramidal cells as well (Royer et al.,

2010). Examples of temporal CA3 pyramidal cell coding of non-spatial information include differentiating open from closed arms on a radial maze and also differentiating radial arm maze traversals toward and away from the reward at the end of the arm (Royer et al., 2010). These two examples suggest that emotional and goal related information is being represented in temporal CA3, which is not a property found in septal HPC cells.

Just as little work has focus on single cell recordings outside of septal HPC, scant information is available about theta and gamma in more temporal levels of HPC. Early reports on the behavioral correlates of theta oscillations in septal HPC noted its prominence during REM sleep and exploratory behaviors (locomotion, whisking etc.; Vanderwolf, 1969; Sainsbury, 1970; Whishaw, 1972; Whishaw and Vanderwolf, 1973; Feder and Ranck, 1973), but variability in the attributes of theta exist even within a particular behavioral state. Investigations into the relationship between locomotor behavior and the amplitude of theta oscillations quickly revealed that the amplitude of theta oscillations in septal hippocampus increases with increases in the running speed of the animal (Teitelbaum and McFarland, 1971; McFarland et al., 1975). This variation in theta power resulting from changes in locomotor activity led both Vanderwolf (1971) and McFarland et al. (1975) to emphasize the importance of controlling for the behavior of the animal when investigating the relationship between theta and cognitive functions. In addition to the amplitude of theta oscillations, theta frequency has also been shown to increase as a function of running speed (Rivas et al., 1996; Slawinsha and Kasicki, 1998; Shin and Talnov, 2001;

Bouwman et al., 2005). Each of these studies looked at theta recorded from the septal portion of the hippocampus and it was not until recently that there was a report on the relationship between theta and running behavior at even a midseptotemporal level of the hippocampus (Maurer et al., 2005). Maurer et al. (2005) suggested that the modulation of theta amplitude by the running speed of a rat decreased at mid-septotemporal levels of CA1 compared to septal levels of CA1, but the lack of simultaneous recordings at septal and midseptotemporal sites and the fact that no statistically significant change in the slope of the speed versus theta amplitude relationship (statistical significance was only found for the ratio of the slope to mean amplitude and ratio of the slope to intercept) leaves this report merely suggesting a change in the speed modulation of theta power along the septotemporal axis.

Chapter 2

Introduction

The laminar organization of the hippocampus (HPC) provides an ideal anatomy for the generation of large amplitude local field potentials (LFPs). Theta (6-12 Hz) LFP oscillations are generated by the summation of synchronous excitatory and inhibitory potentials as well as intrinsic membrane oscillations (eg, Green & Arduini, 1954; Petsche et al., 1962; Leung, 1985; Brankack et al., 1993; Bragin et al., 1995; Buzsaki, 2002; Montgomery et al., 2009). A number of studies have linked changes in theta to cognitive variables in several mammalian species (eg, Ulanovsky & Moss, 2007; Rizzuto et al., 2006; Montgomery et al. 2009) while variation in the theta signal in the rodent has often been linked to locomotor speed and sensorimotor integration (see Bland and Oddie, 2001 and Sinnamon, 2006 for excellent reviews).

Early reports on the behavioral correlates of theta noted its prominence during locomotor behavior and the obvious relationship to running speed (Vanderwolf, 1969; Teitelbaum and McFarland, 1971; Whishaw and Vanderwolf, 1973; Feder and Ranck, 1973;; McFarland et al., 1975). The variation in theta resulting from changes in locomotion led both Vanderwolf (1971) and McFarland et al. (1975) to emphasize the importance of controlling for the behavior of the rat when investigating the relationship between theta and cognitive functions. The increase in theta power in relation to running speed has been confirmed in a number of studies examining the septal pole of the HPC (Rivas et al., 1996;

Slawinsha and Kasicki, 1998; Shin and Talnov, 2001; Bouwman et al., 2005). Maurer and colleagues (2005) suggested variability in the role of speed at more temporal (mid-septotemporal sites) aspects of the HPC, while several reports have minimized the relative importance of locomotor speed in relation to theta power (eg, Montgomery et al. 2009).

There is considerable septotemporal variation in afferent input to the HPC. Inputs from the entorhinal cortex (EC) define three segregate domains along the septotemporal or long axis based upon the band of origin in the EC (Dolorfo and Amaral, 1998; Witter, 2007; see Fig 1). Subcortical neuromodulatory input from cholinergic, serotonergic and noradrenergic inputs exhibit variation across the septotemporal axis (Amaral and Kurz, 1985; Gage and Thompson, 1980; see also Thompson et al, 2008 for review), while a prominent amygdala input preferentially targets the temporal levels of the HPC (see Pitkanen et al., 2000 for review).

The present study examined the relationship between running speed and various measures of theta across the septotemporal axis of both CA1 and DG, as well as in EC. We demonstrate that locomotor speed is a prominent predictor of theta power and coherence in the septal-most aspect of the HPC and that there is systematic decrease in the relationship between speed and theta indices, including theta coherence, at more temporally located electrode sites. Further, we observed decreases in theta power over repeated testing within multiple daily sessions at more temporally located electrode sites without any decrement in theta power at septal HPC sites. These habituation related decreases at more

temporal sites were unrelated to locomotor speed, These results are discussed with regards to anatomical features that may underlie differences across the septotemporal axis as well as the dynamism of theta and gamma measures as indices of neural network function.

Materials and Methods

Animals and Surgical Procedures

Six adult male Fisher-344 rats were used in this study. The animals were individually housed in a temperature-controlled room and maintained on a 12-h/12-h light-dark cycle. All procedures were performed in accordance with the guidelines set forth by University of Connecticut's Institutional Animal Care and Use Committee and NIH.

Rats were anesthetized with a ketamine cocktail (4 ml/kg) consisting of (in mg/ml): 25 ketamine, 1.3 xylazine, and 0.25 acepromazine. After a midline scalp incision, burr holes were drilled in the skull over the hippocampus and three electrode arrays were positioned along the septotemporal extent of the HPC, while a fourth array was positioned in the entorhinal cortex. The following coordinates were used for each of the four arrays: Septal HPC (AP -3.0, ML 2.5, DV 3.0); Intermediate HPC (AP -5.0, ML 5.0, DV 5.0); Temporal HPC (AP -6.5, ML 5.5, DV 7.0); Entorhinal Cortex (AP -8.0, ML 6.5, DV 6.5 - 7.5). Each electrode array consisted of four linearly spaced 50 μ m tungsten wires (16 total electrodes; California Fine Wire Co., Grover Beach, CA), arranged and spaced using fused silica tubing (Polymicro Tubing, Phoenix, AZ). All electrodes were attached to female pins (Omnetics, Minneapolis, MN) secured in a rectangular five by four pin array. Two stainless steel watch screws driven into the skull above the cerebellum served as indifferent and ground electrodes. Two or more additional support screws were positioned over the anterior aspect of the skull

and the entire ensemble was secured with dental acrylic. Rats were allowed to recover for one week following surgery.

Electrophysiological Recordings, Data Acquisition and Behavior

Wide-band electrical activity was recorded (1-2000 Hz, 3787 samples/sec) using a Neuralynx data acquisition system (Bozeman, MT). Electrophysiological recordings occurred during the light phase of the light/dark cycle and were obtained while rats shuttled between ends of a linear track (10 X 140 cm) for chocolate sprinkles. Light emitting diodes attached to the headstage were tracked via a camera (33 samples/sec) positioned over the linear track, thus allowing for an offline record of the animals position over time. In order to calculate the rats speed, the positional difference between successive tracking samples was calculated and then lowpass filtered in order to minimize the contribution of head movements to the overall speed of the rat. The result was used to calculate mean speed during designated intervals (see below).

Rats were food deprived to 85% of their ad libitum weight and trained to run on a linear track for chocolate sprinkles. Recording sessions consisted of five individual recordings separated in time within a single day. The end of the first recording marked Time 0 (T0). The subsequent four recordings were initiated at +5, 20, 60 and 120 minutes. Each of the five recordings required the rat to complete a minimum of 50 trials, where a single behavioral trial consisted of the rat running from one end of the track to the other end. After the rat

completed 50 trials, it was returned to its home cage on a table adjacent to the linear track until it was time to start the next recording. No changes were made to the track or the room in between recordings.

Data Analysis

All data analysis was conducted using custom written programs in MatLab (The MathWorks, Natick, MA). The following criteria were applied to the acquired dataset in order to restrict all analyses to movement related data. Two criteria were set in order to identify the beginning of each trial: 1) a physical threshold 14 cm from the beginning end of the linear track and 2) a speed greater than 5 cm/sec. These criteria ensured that data from when the rat was turning around after consuming the food reward was not included in the analysis. The end of the trial was identified as the point in time when the rat passed another physical threshold 14 cm from the other end of the track. Additionally, any trial during which the rats speed decreased below 5 cm/sec between the beginning and end of the trial was discarded. The resulting dataset contained an average of 46.4 +/- 0.88 (SEM) trials per recording.

Power Spectral Density

Power spectral density estimates were obtained using Welch's averaged modified periodogram method (Welch, 1967) for the last 1.5 seconds of each trial. The integrated power for theta (6-12 Hz) was calculated from the power

spectral density. The resulting power values, along with the corresponding mean speeds for each trial, were subjected to a linear regression analysis (see below for more details).

Coherence

Trials were sorted based on mean speed and then the EEG signals from each channel were concatenated into a single continuous string of data (Roark and Escabi, 1999, see Sabolek et al., 2009 for a detailed description), such that each recording generated a series of twenty second long data strings with different mean speeds associated with each of them. The slowest trials totaling twenty seconds were concatenated, the next slowest totaling twenty seconds were concatenated and so forth for all trials. Coherence values (Bullock et al., 1990) for each channel pair were computed using the Welch periodogram estimation procedure with a spectral resolution of ~ 2 Hz. Coherence is a measure of the linear association between two signals as a function of frequency. A significance estimation procedure was devised in which the coherence estimate was compared to that of signals with identical magnitude spectrum but with zero phase coherence. For each channel pair, the cumulative distribution of the frequency- dependent coherence values was created by circularly phase shifting one signal in the pair by a random amount, calculating the coherence for the shifted signals, and bootstrapping the procedure 250 times (Efron and Tibshirani, 1993). This procedure guarantees that the signal spectrums are identical but have no linear association, because the phase or time information

has been removed. The coherence distribution was used to determine a threshold for each frequency band (2 Hz resolution), below which 95% of the shifted null hypothesis coherence values fell. Thus, only regions of the non-shuffled signal coherences falling above the 95% threshold were considered significant. For each channel pair, the statistically significant area in the theta (6-12 Hz), and gamma (40-100 Hz) ranges were calculated, and normalized by the frequency range (expressed as average coherence value per Hz) to facilitate comparison of different frequency ranges. The coherence value was then normalized for band width and a new zero point, the resulting normalized coherence value falls between 0 and 1.

Statistics

Each spectral index from each electrode was separately subjected to a simple linear regression analysis that included the mean speeds and the spectral index for the corresponding period of time in order to assess the relationship between locomotor speed and each of the spectral indices. Thus each electrode/electrode pair yielded a single correlation coefficient (r-value) for each spectral index. Each individual quartile of DG and CA1, as well as MEA and LEA, were separately tested to determine whether that region had a mean r-value different than zero using a T-test. A non-zero mean for a region's speed r-value distribution indicates that that spectral index is significantly speed modulated either positively or negatively (Lorch and Myers, 1990). Additionally a simple linear regression analysis was conducted on the speed r-values for DG

and CA1 along with the distance from the septal pole (in mm) as an explanatory variable, thus demonstrating whether the speed modulation of each spectral index varied along the septotemporal axis.

In order to assess any changes in theta power over the repeated recordings, a linear regression analysis was conducted that included the mean speeds and four orthogonal dummy coded variables for the five recording timepoints as explanatory variables. Each electrode yielded a single standardized regression coefficient (β -value, where $\beta = b \frac{SD_x}{SD_y}$) for each of the explanatory variables. The resulting distributions of β -values were then individually tested for each quartile of DG and CA1, as well as MEA/LEA, to determine whether that region had a mean different than zero using a T-test. The β -values for each of the dummy coded variables indicate how theta power changes in relation to the baseline recording while controlling for speed. Thus a significant non-zero mean for a region's β -value distribution indicates that theta power increased/decreased significantly from baseline (controlling for the influence of speed). A repeated measures ANOVA was also conducted on the β -values from each quartile of DG and CA1, as well as from MEA/LEA, for the different recording timepoints in order to assess whether there was an effect of time on theta power.

Histology

Following the completion of recordings, rats were anesthetized with Euthasol (sodium pentobarbital solution) and transcardially perfused with ice-cold

saline followed by 4% paraformaldehyde in 0.1M phosphate buffer (pH 7.2). Brains were sliced (50 μ m sections) using a vibratome (Vibratome Series 1500), mounted, and Nissl stained using thionin. All electrode positions were verified and categorized according to laminar and septotemporal position. Septotemporal distances between electrode positions were determined by noting the location of each electrode position on a flatmap representation of the HPC (Swanson, 1978). Each section of a flatmap represents approximately 200 μ m of tissue, and so fairly accurate approximations of the relative distance between electrodes could be determined by counting the number of sections between two electrodes. Photomicrographs of relevant electrode tracks were captured using a Nikon microscope connected to a Spot RT camera system, digitized and prepared for presentation using Adobe Photoshop 7.0.

Results

Electrodes were positioned at sites primarily within stratum moleculare or stratum granulosum of the DG (N = 15), while CA1 (N = 25) sites spanned from the ventral aspect of stratum pyramidale to stratum lacunosum moleculare with the majority of sites within stratum radiatum (see Figure 2A). In the areal direction, DG placements ranged from 1.6 – 4.8 mm from the septal pole (within the septal and mid-septotemporal regions), while placements in CA1 ranged

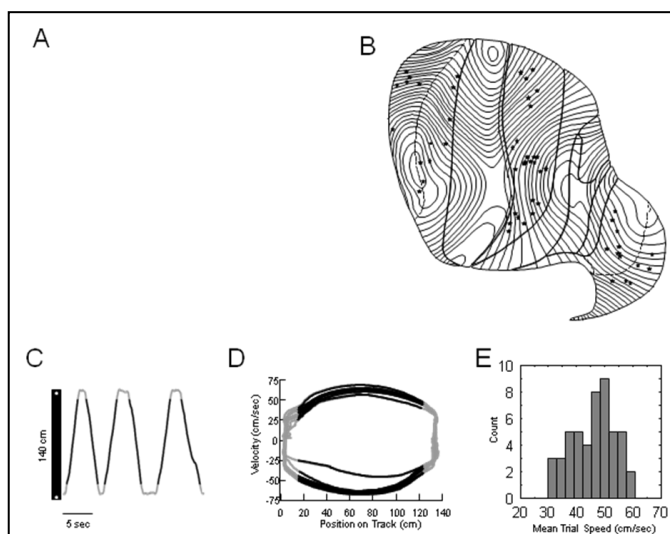


Figure 2. **A)** Photomicrographs of representative recording sites. **B)** Flatmap representation of the hippocampal formation with all recording locations indicated by black stars. The septal pole of the hippocampus is located at the top and the temporal pole at the bottom. **C)** Position of a rat along the 140 cm linear track during six consecutive trials. Black lines overlaid on the grey trace indicate portion of each track traversal that was considered as an individual trial. **D)** The rats velocity as a function of position on the track is shown. Again the black lines indicate the portion of each traversal that was included as a single trial in further analyses. **E)** Distribution of mean trial speeds for a single recording.

more broadly from 1.3 – 7.6 mm from the septal pole. Electrode placements within the superficial layers of the EC included sites in the medial (n = 7) and

lateral (n = 6) subdivisions that were dispersed across lateral, intermediate and medial bands (Figure 2B).

At all electrode sites, visual inspection and power spectral density confirmed the presence of theta oscillations while rats shuttled between ends of a linear track for food reward (Figure 2C). The power of theta varied according to laminar position as has been well described in the septal HPC (see Bragin et al., 1995) with sites nearest the hippocampal fissure within stratum molecular of DG and stratum lacunosum moleculare of CA1 yielding the largest amplitude signals.

We observed a slight decrease in theta power of roughly 3-5 dB when

Table 1: Theta by HPC Quartile and within LEA/MEA

	CA1-Q1	CA1-Q2	CA1-Q3	DG-Q1	DG-Q2
Baseline (Mean + SEM)	46.3 ± 2.2 [*]	40.1 ± 1.4	40.7 ± 1.0	40.3 ± 0.8	37.1 ± 1.9
Baseline (Range + SEM)	6.2 ± 0.9	7.5 ± 0.4	7.2 ± 0.6	7.9 ± 0.7	9.0 ± 0.4
	MEA	LEA			
Baseline (Mean + SEM)	33.5 ± 1.1	32.4 ± 1.1			
Baseline (Range + SEM)	9.6 ± 0.8	10.3 ± 1.1			

Baseline values expressed as dB relative to 1μV.

¹ CA1 sites within the 1st quartile of septal HPC had significantly more power in the theta band (p < 0.05) when compared to CA1 sites within either 2nd or 3rd quartiles. No differences were observed in baseline theta values across quartiles within the DG or across MEA vs LEA sites.

comparing sites in the septal most quartile (both DG and CA1) to sites in

homotopic positions in the second and third quartiles (Table 1, Figure 3A). To some extent the difference in theta power may reflect anatomic differences in the

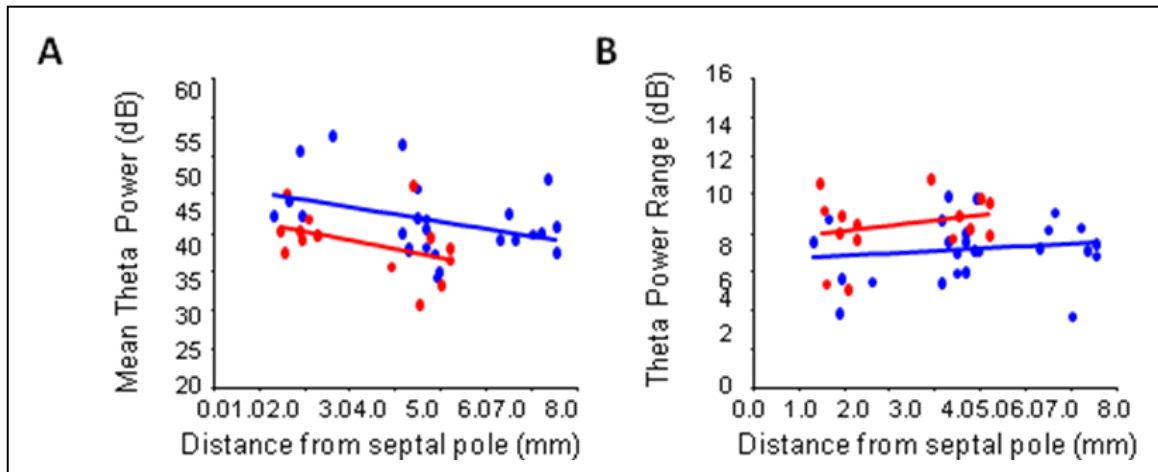


Figure 3. **A)** Baseline theta power values as a function of distance from the septal pole. Theta power tended to be slightly lower in both CA1 and DG with greater distance from the septal pole. **B)** Despite the lower theta power values with greater distance from the septal pole, the range of values at a given site did not vary as a function of distance from the septal pole.

density of afferent inputs involved in the generation of these field potentials and/or the density of the dendritic fields in which those afferents terminate. Despite the differences in absolute power, the dynamic range of theta power (~6 – 10 dBs) did not vary across the septotemporal axis of either DG or CA1 (Table 1, Figure 3B).

Increase in theta power in relation to locomotor speed varies across the septotemporal axis

All electrode sites located in the septal-most HPC exhibited a prominent increase in theta power as a function of running speed. Initial visual inspection of the relationship between speed and theta power for all electrodes within a given

animal illustrated the clear variation in this relationship throughout the hippocampal formation (Figure 4B, 5A,D). Examples from two rats show the relationship between speed and theta power from simultaneously recorded electrodes at two septotemporal levels of CA1 and DG, as well as in EC (Figure 4B) and also at three simultaneously recorded sites along the septotemporal axis of CA1 (Figure 5A).

Thus, speed accounted for a significant portion of the variability in theta power at the septal most electrode sites, while sites located more temporally in

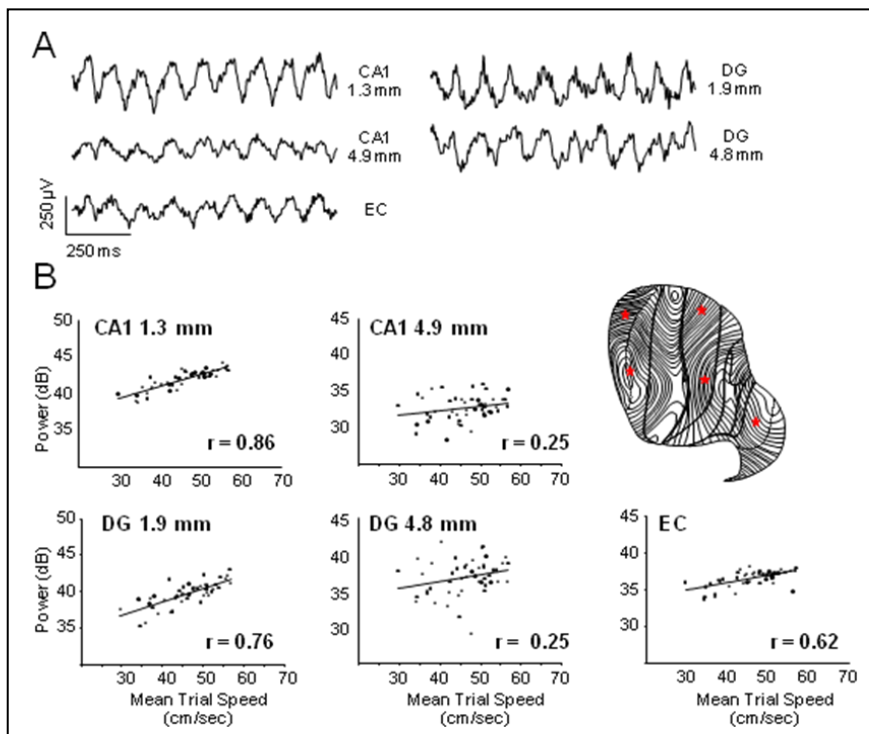


Figure 4. A) Local field potential traces simultaneously recorded from two septotemporal levels of CA1 and DG, as well as one site in EC from a single rat. Note the prominent theta oscillations present at all recording locations. The distance from the septal pole is indicated for the CA1 and DG recording sites. B) Each scatter plot shows the

relationship between mean trial speed and theta power for the five simultaneously recorded sites shown in A). The distance of the CA1 and DG recording sites from the septal pole are displayed at the top of each plot and the correlation coefficient (r) is displayed at the bottom of each plot. Note the strong relationship between speed and theta power at the septal CA1 and DG sites, as well as the EC site, but that the relationship decreases at the more temporal sites. On the right is a flatmap representation of the hippocampal formation with the red stars indicating the five recording locations.

each individual animal exhibited a clear decrease in the relationship between speed and theta power. In order to quantify this change along the septotemporal

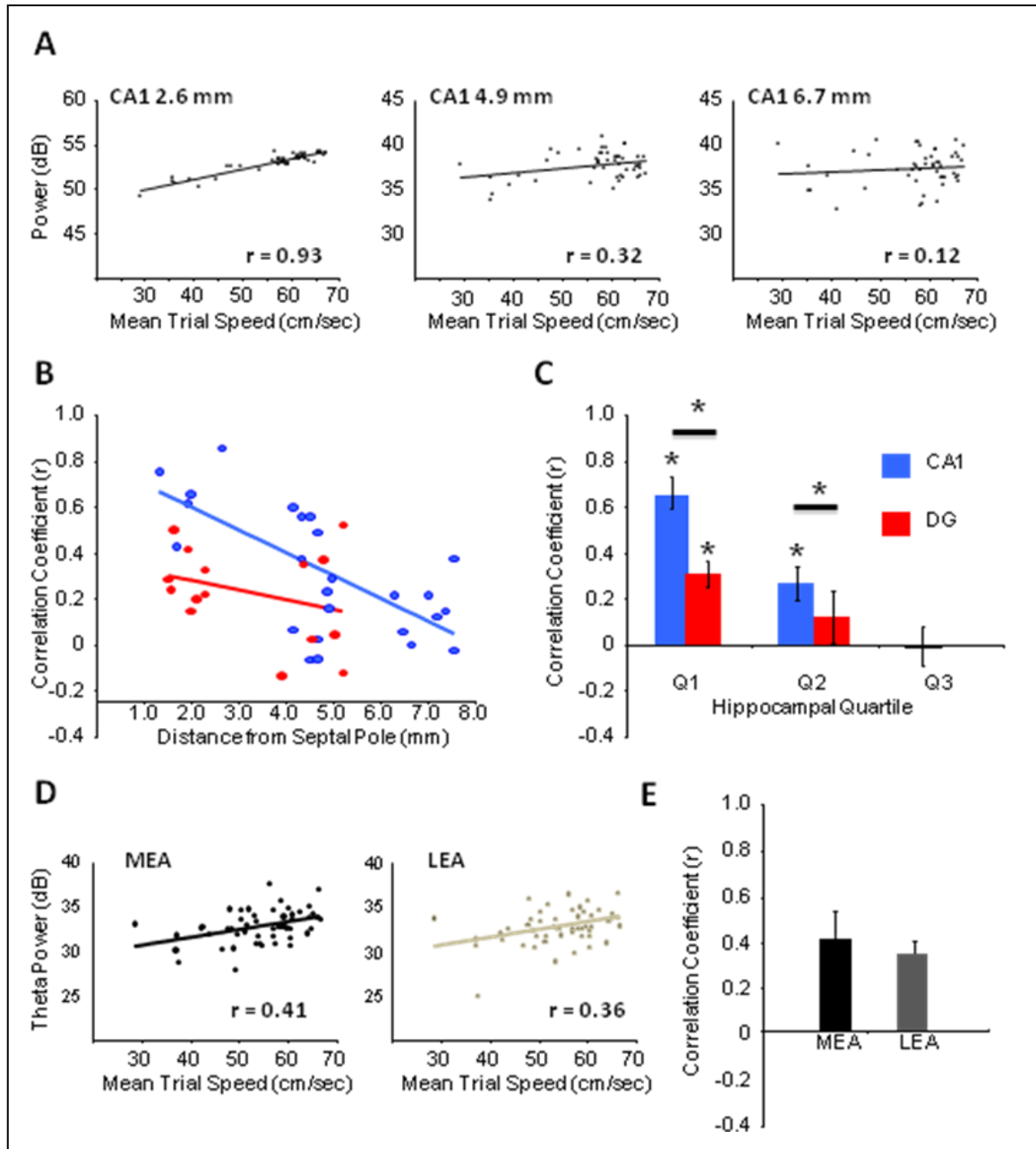


Figure 5. **A)** The scatter plots show the relationship between mean trial speed and theta power for three simultaneously recorded sites along the septotemporal axis of CA1. The distance of each recording site from the septal pole is displayed in each plot along with the correlation coefficient. Note the decrease in the correlation coefficients with increasing distance from the septal pole. **B)** The relationship between distance from the septal pole and the speed vs theta power correlation coefficients for each CA1 and DG

electrode is shown in the scatter plot. A significant decrease in the CA1 correlation coefficients as a function of distance from the septal pole can be seen (blue), while there was a trend for a decrease in DG (red). **C)** All CA1 and DG electrodes were grouped according to septotemporal quartile in order to assess whether theta power was significantly speed modulated in each region. Theta power was significantly speed modulated in the first and second quartiles of CA1, but only in the first quartile of DG. Additionally, there was greater speed modulation of theta power in CA1 than in DG. **D)** Scatter plots, as in A), of the relationship between mean trial speed and theta power for two simultaneously recorded electrode sites in EC, with one site in MEA and the other in LEA. **E)** Mean correlation coefficients for MEA and LEA. Theta power was significantly modulated by speed in both areas.

axis of DG and CA1, we analyzed the data two ways. First, we conducted a correlational analysis using the septotemporal position of the electrode (millimeters from septal pole) and the corresponding r-value (speed vs power) for that electrode. The relationship of speed to theta power significantly decreased along the septotemporal axis of CA1 ($N = 25$, $r = -0.69$, $p < 0.0005$; Figure 5B). While there was a clear trend for a decrease in the relationship of speed to theta power along the septotemporal axis of the DG, this relationship was not significant ($N = 15$, $r = -0.38$, $p = 0.16$; Figure 5B). DG sites did not extend beyond roughly 5 mm from the septal pole and no DG sites were located in the temporal 50% of the HPC (Figure 2B, 5B). While the speed modulation of theta power displayed a decrease along the septotemporal axis, this does not demonstrate whether sites at more temporal levels exhibited a significant relationship between speed and theta power. In order to determine whether theta power at different septotemporal levels of DG and CA1 was significantly related to speed, we grouped electrodes for each HPC quartile and conducted t-tests on the distribution of correlation coefficients (r-values). A significant relationship between theta power and speed was observed for electrode sites within the first

two quartiles of CA1 (1st: $t(4) = 9.25$, $p < 0.001$; 2nd: $t(11) = 3.79$, $p < 0.005$), but not for electrode sites in the third quartile (3rd: $t(7) = -0.08$, $p = 0.94$; Figure 5C). In DG, a significant relationship between speed and theta power was observed only for electrode sites in the septal most quartile (1st: $t(7) = 5.71$, $p < 0.001$; 2nd: $t(6) = 1.04$, $p = 0.34$; Figure 5C).

Thus, a positive linear relationship between speed and theta power was quite evident in all septal (1st quartile) electrode sites with speed accounting for considerable variation in theta power at both CA1 (mean r-value for CA1 sites in 1st quartile = 0.66 ± 0.07) and DG (mean r-value for DG sites in 1st quartile = 0.31 ± 0.05) sites. Notably, locomotor speed accounted for more of the variability at CA1 sites than at DG sites within the first and second quartiles of the HPC (p 's < 0.001 ; Figure 5C).

Habituation of theta power across sessions varied across the septotemporal axis

We collected data during an initial run session (baseline) of at least 50 trials and then returned rats to the linear track to run additional sessions of at least 50 trials at 5, 20, 60 and 120 minutes after the end of the initial run session. In examining data across repeated recording sessions within a single day, it became obvious that there was a systematic decrease in theta power over

sessions at more temporally located electrode sites. A clear downward shift in the linear best-fit line for the relationship between speed and theta power was

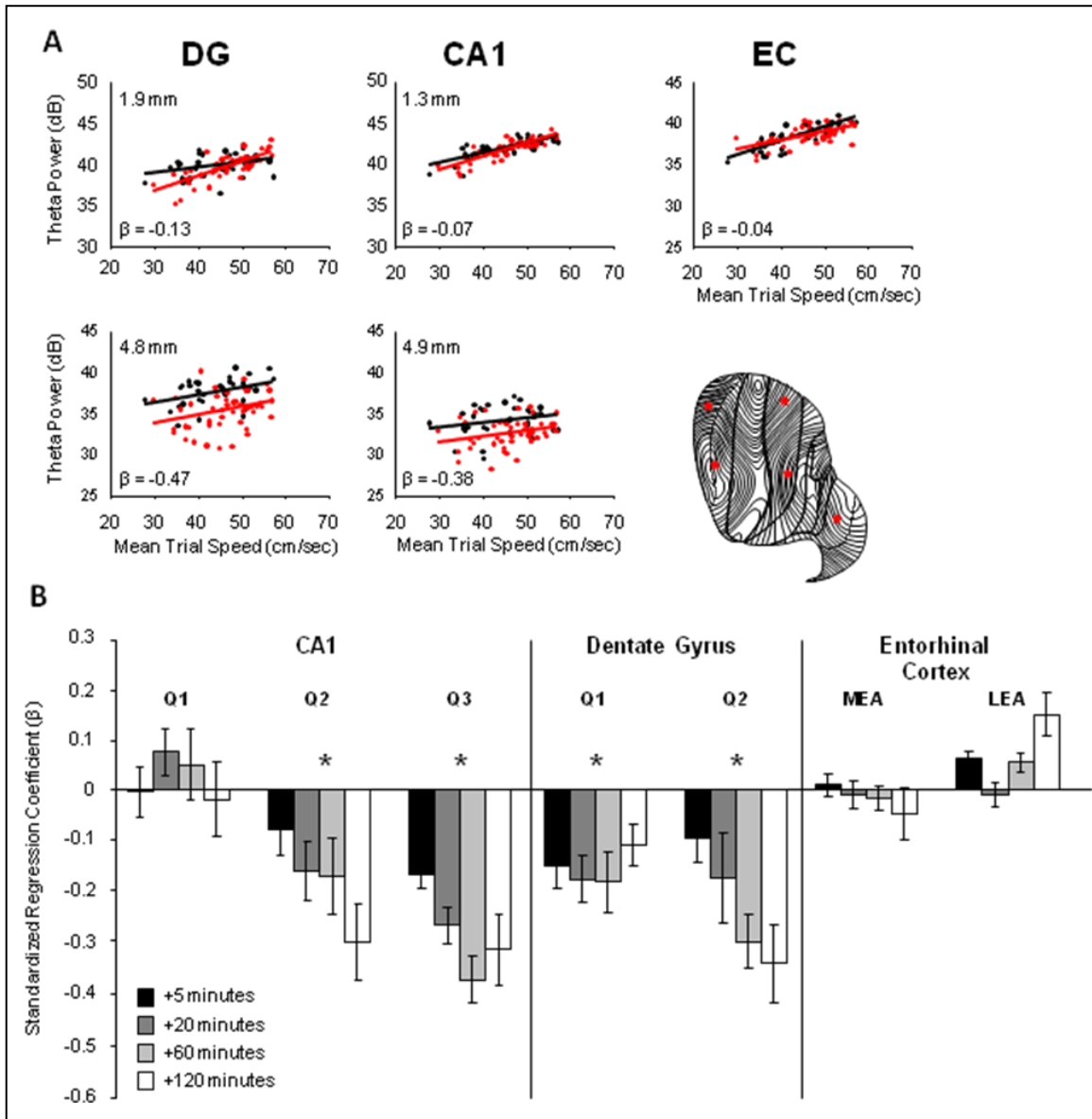


Figure 6. **A)** Flatmap displays five simultaneous recording sites (same as in Figure 2). Scatter plots show theta power as a function of mean trial speed during the baseline recording (black) and the fifth recording session of the day that was initiated 120 minutes after the cessation of the baseline recording (red). The distance from the septal pole is indicated for the hippocampal sites, as well as the standardized regression coefficients (β) for each site. A clear downward shift in the linear best fit line can be seen in the more temporal DG and CA1 sites demonstrating a within day habituation of theta power. **B)** Mean β -values for all regions investigated. There was a significant effect of time in the second and third quartiles of CA1 and the second quartile of DG, while the first quartile of DG showed a decrease in theta power without an effect time.

observed at the more temporal aspects of both DG and CA1 without any significant change in the slope of the lines (Figure 6A). This shift was not evident at septal HPC sites (Figure 6A). In order to examine if this decrease had any relation to running speed or time (habituation), we conducted a linear regression analysis, factoring out speed across time points. The resulting β -values were then assessed using a within-electrode repeated measures ANOVA. A significant time-dependent reduction in theta power was observed in the second and third quartiles of CA1, as well as within the second quartile of the DG (CA1 Q1 $F(3,12)=3.49$, $p=0.05$; CA1 Q2 $F(3,33)=12.08$, $p<0.001$; CA1 Q3 $F(3,21)=6.99$, $p<0.005$; DG Q1 $F(3,21)=1.76$, $p=0.19$; DG Q2 $F(3,18)=7.58$, $p<0.005$; Figure 6B). A significant decrease in theta power was observed among electrodes in the first quartile of the DG ($p < 0.01$; Figure 6B), but this decrease did not vary across time points. No significant changes were observed among electrodes in the first quartile of CA1 (Figure 6B).

Thus the reduction in theta power observed at more temporally located recordings sites appears to represent habituation to sensory, motor or motivational aspects of the behavior without any obvious relationship to differences in the overt motor act (eg, speed of locomotion). Wyble and colleagues (2004) have previously observed a decrease in theta power, time-locked to lever pressing in the septal HPC.

Summary of changes in theta power as a function of speed and habituation

Thus, 1) locomotor speed predicts a considerable amount (~30-60%) of the variability in theta power at CA1 sites in the septal most quartile of the HPC; 2) locomotor speed is more predictive of changes in theta power at CA1 sites compared to DG sites even at the most septal electrode locations; 3) there is a prominent decrease in the relationship of speed and theta power at both CA1 and DG sites at more temporal levels of the HPC; 4) there is a decrease in theta power over repeated sessions of running within a day at more temporal sites in HPC, while this phenomenon was not observed at septal CA1 or EC sites.

Theta indices within the entorhinal cortex

Theta LFP's were recorded at 13 electrode sites within the superficial layers of the EC in both the medial ($n = 7$) and lateral ($n = 6$) subdivisions of the EC (Fig 2B). The power of theta signals from both MEA and LEA were moderately lower than those observed in the HPC, but no differences were observed between MEA and LEA sites (see Table 1).

Sites in both MEA and LEA showed significant speed modulation of theta power (MEA: $t(6) = 3.81$, $p < 0.01$; LEA: $t(5) = 15.10$, $p < 0.0001$) with no difference between MEA and LEA sites ($t(11) = 1.09$, $p = 0.30$; Figure 5D,E). Locomotor speed predicted roughly 10-20% (mean $r^2=0.18$ for all EC sites) of variability at electrodes sites in the MEA and LEA. Thus the relationship of speed

to theta power was less than that observed at septal HPC sites, suggesting that the relationship of speed to theta power within septal HPC sites is not a consequence of this phenomenon at EC sites.

Rhinal-Hippocampal and Intrahippocampal Theta Coherence

A few studies have characterized theta coherence between hippocampal and entorhinal sites and variation in relation to theta state and behavior. We have examined theta coherence between the HPC and EC in the rat and have found no significant changes in theta coherence between the HPC and EC during running and REM sleep (Chrobak, personal observations). In the present study the relation between locomotor speed and theta coherence was examined between EC and DG sites (EC-DG pairs = 32) as well as CA1 (EC-CA1 pairs = 48). Similar to changes in theta power, theta coherence between paired EC and HPC sites significantly increased as a function of locomotor speed when the pair included a septal HPC electrode site (Figure 7A).

Correlational analysis of the septotemporal position (distance from septal pole) and the speed-related r-value showed that theta coherence between EC-CA1 pairs and EC-DG pairs exhibited less relation to speed when HPC electrodes sites were located at more temporal levels ($r = -0.44$, $p < 0.005$ for EC-CA1 pairs; $r = -0.55$, $p < 0.005$ for all EC-DG pairs regardless of areal position of the EC electrode (see Figure 7B). Examining the data grouped by hippocampal quartiles, theta coherence increased in relation to locomotor speed

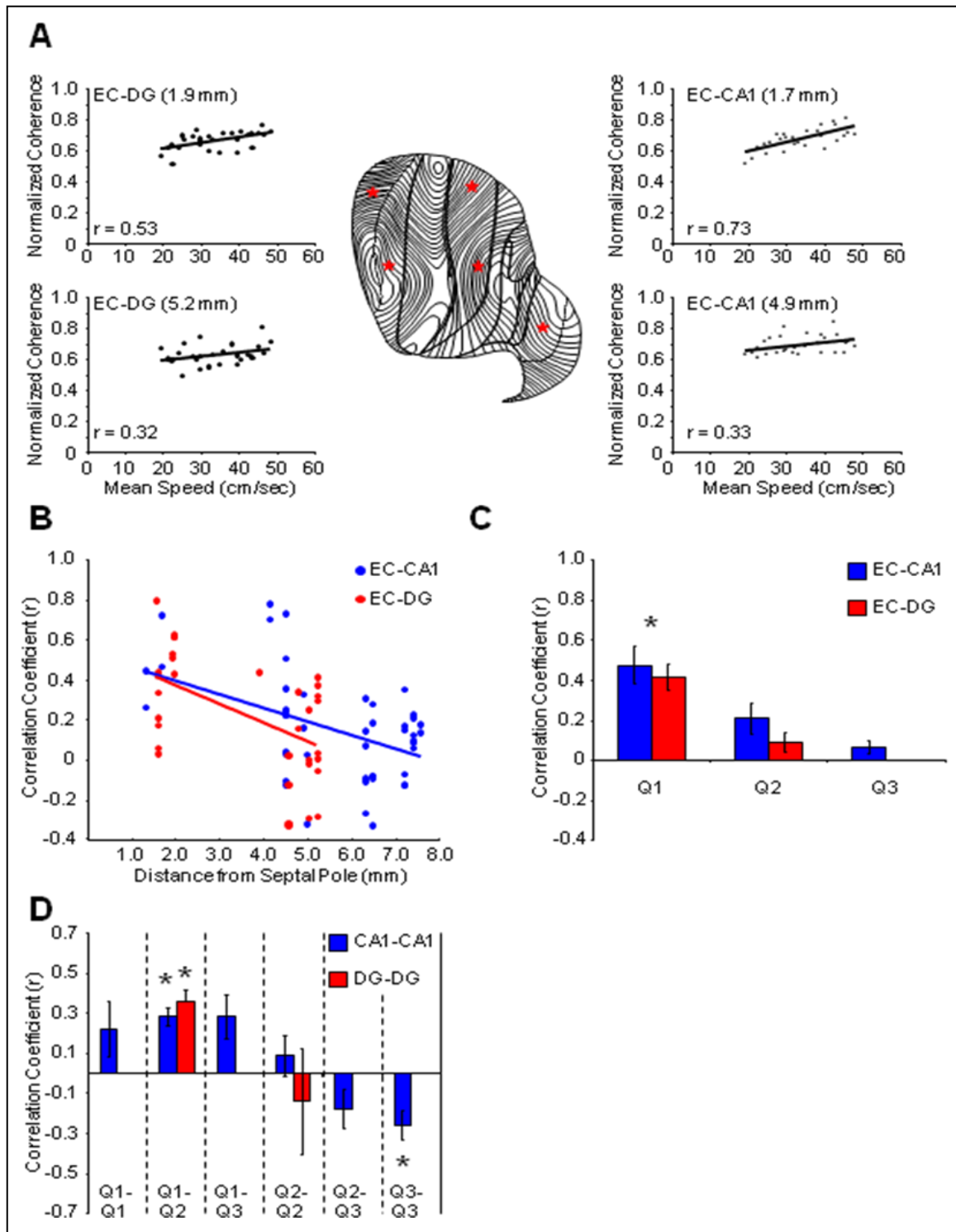


Figure 7. A) Middle, flatmap showing a recording site in EC and four hippocampal sites. Scatter plots show the relationship between mean trial speed and theta coherence between

the EC site and the four different hippocampal sites. Distances displayed in each plot are the distance of the hippocampal electrode sites from the septal pole. Also displayed in each plot is the correlation coefficient for the relationship between speed and theta coherence for that electrode pair. Note that theta coherence between EC and the more temporal hippocampal electrodes is less speed modulated than theta coherence between EC and the septal hippocampal electrodes. **B)** The speed modulation of EC-CA1 (blue) and EC-DG (red) theta coherence significantly decreases as a function of the distance from the septal pole of the HPC electrode. **C)** Theta coherence between EC and the first quartile of CA1 and DG is speed modulated, while theta coherence between EC and all other quartiles is not speed modulated. **D)** Theta coherence within the hippocampus is speed modulated when the electrodes are within the septal half, while theta coherence within more temporal aspects of CA1 actually decreases with increasing locomotor speed.

only between EC-CA1 and EC-DG pairs within the septal most quartile of the HPC (EC-CA1 ($t(3) = 5.04$, $p = 0.02$; EC-DG ($t(12) = 6.30$, $p < 0.0001$; Figure 7C). Thus the speed-related increase in theta coherence between any EC electrode and any HPC electrode varied along septotemporal axis.

Importantly, the intrahippocampal coherence in relation to speed also exhibited variation along the septotemporal axis. Plotting the speed-related correlation coefficient among HPC electrode pairs by quartile, Figure 6D illustrates that coherence among the septal most electrodes increased, while coherence among more temporally located pairs decreased as a function of locomotor speed.

DISCUSSION

Theta signals within the hippocampal formation (HPC and EC) may reflect alterations in locomotor speed, sensorimotor integration, the flow of sensory input, or cognitive operations (eg, Bland and Oddie, 2001, Kay, 2005; Ulanovsky and Moss, 2007; Montgomery et al., 2009; Nyhus and Curran, 2010). Systematic analyses of theta LFP signals provides a unique intermediate window into the systems-level function of hippocampal networks, filling the temporal and spatial gap between the discrete-sensory related discharge of isolated neurons (eg, place cells) and wholesale activation of neural tissue observed using functional neuroimaging techniques. Much is known about the cellular and circuit physiology that contributes to local theta oscillations as well as the general relationship of theta to global states of behavior (see Buzsaki, 2005 and Buzsaki and Draguhn for reviews). However, there is quite limited information about the variables that govern, and the mechanisms that support theta synchronization across brain regions (see Raghavachari et al., 2006).

The present findings demonstrate substantial septotemporal variation in the relationship between locomotor speed and indices of theta LFP's within the HF of the rodent. Foremost, we observed that theta power increased linearly as a function of speed at electrode sites in the septal HPC, accounting for 40-60% of the variability in the power of the theta signal. The strength of this relationship diminished substantially with distance from the septal pole. The relationship of speed to theta power and the decline across the septotemporal axis was more

prominent at CA1 sites as compared to sites within the DG. Second, we observed significant changes in theta power as a function of behavioral habituation (repeated runs on a linear maze). This decrease in theta power was minimal at CA1 sites in the septal HPC, and was most striking at sites located distant from the septal pole. Third, theta power increased linearly with speed at all EC sites, including both LEA and MEA sites. The relationship between speed and theta power did not vary across the area axis of the EC (LEA as compared to MEA). Fourth, theta coherence between EC and HPC also exhibited septotemporal gradient in its speed relationship, such that coherence between EC-septal HPC sites was positively speed modulated, while coherence between EC – temporal HPC sites was not speed modulated. The latter suggests that in relation to speed, there is regional segregation in synchronization between HPC and EC. Last, theta coherence increased as a function of speed across pairs of septally-located electrodes, while theta coherence decreased across more temporally located pairs. Thus in relation to speed alone, there was an increased synchronization between sites located in septal HPC, while decreased synchronization between septal and more distant sites in the temporal HPC. Generally, with increasing locomotor speed there are regionally select changes in theta across the septotemporal axis of the HP that suggest septotemporal-specific differentiation of interacting neural ensembles.

Our most basic finding is that speed was a prominent predictor of theta indices in the septal HPC accounting for 40-60% of the variability in theta power at septal CA1 sites. However speed had limited relation to the variation in theta

power observed at more temporally located CA1 and DG sites. This difference was not attributable to a decrease in the dynamic range of the theta signal, but likely reflects a fundamental difference in the mechanisms that govern theta and the discharge of hippocampal neurons across the septotemporal axis. Two points are of particular note. First, while locomotor speed has been demonstrated to be a key player in variation in theta power in the rat, various studies suggest that speed is not always a particularly relevant factor (eg, Montgomery et al., 2009 and one other). While the present data set cannot account for observed differences, the present study demonstrates that subtle deviations in areal position influence the relation of speed to theta power and that there are significant changes over repeated behavioral testing within a daily session. Importantly, the recent experience of the animal seems to play a fairly significant role in the dynamism of theta signals within the HPC. What these data suggest is that theta is a highly dynamic signal reflecting clear variation in the septotemporal synchronization of synaptic input across the dendritic field of hippocampal neurons that likely changes with minimally recent behavioral experience and ongoing sensorimotor experience.

Anatomic differences across the septotemporal axis

The areal variation in theta signals likely reflects variation in the topography of several afferent inputs that synapse on the dendritic field of CA1 and DG neurons. There are three major populations of excitatory glutamatergic

afferents that are critical to theta current generation. First, projections from layer 2 EC neurons target the distal dendrites of dentate granule neurons (as well as local GABAergic neurons). Second, projections from layer 3 EC neurons target the distal dendrites of CA1 neurons. These EC projections originate from segregate areal bands that project in a topographic manner along the septotemporal axis with the lateral band EC neurons targeting the septal 50% of the HPC (see Fig X: Dolorfo and Amaral, 1998). The medial most band targets the temporal 25% of the HPC. The EC projections thus provide a potential source of variation in the theta signal across the septotemporal axis of the HPC. Third, intrinsic hippocampal associational projections (CA3 to CA1 and mossy cells to DG) project extensively across the septotemporal axis (see Amaral and Witter, 1995) providing a potential mechanism for synchronizing neural activity across the long axis and linking distant neural ensembles.

While the topography of EC afferents could contribute to differences in theta synchronization, there is limited correspondence between the topography of EC inputs and the decrease in the relationship between speed and theta power across septotemporal distance (see Fig X). Basically, lateral band neurons innervate the entire septal half of the HPC and no known topographic pattern distinguishes an EC input to even the septal most quartile as compared to the next quartile. Further, we found no variation in the degree of relationship between locomotor speed and any theta index across the areal surface of the EC, although a more thorough mapping of the relationship of speed to theta power is warranted. On the basis of the present data it does not appear that the

source of variation across the septotemporal axis reflects variation in the EC input. In contrast, any number of studies have pointed to a role for ascending brainstem circuits, which target the HPC directly as well as indirectly via the medial septal nucleus, in regulating hippocampal theta (see Bland and Oddie, 2000; Vertes et al., 2004).

Several subcortical afferents exhibit substantial variation in the density of input across the septotemporal axis. The density of cholinergic, noradrenergic and serotonergic afferents varies across the septotemporal axis (Gage and Thompson, 1980; Amaral and Kurz, 1985). In addition to the more well-known neuromodulatory inputs, excitatory glutamatergic inputs from both the supramammillary nucleus of the hypothalamus exhibit considerable variation in the density of input across the septotemporal axis (Vertes, 1992; Vertes et al., 2006). The supramammillary input exhibits a much denser input to the septal most HPC that preferentially targets the DG, with very sparse input to CA1. This input also provides dense projections to the medial septal nucleus, whose cholinergic, GABAergic and glutamatergic inputs play a key role in orchestrating theta within the HPC and EC (see Lee, 1994; Vertes and Kocsis, 1997).

A long history of research has described the role of ascending subcortical circuits in regulating hippocampal theta (see Vertes and colleagues, 2004). While a number of studies demonstrate the variation in the discharge rate of subcortical neurons across theta states, few studies have systematically defined changes in firing rate as a function of locomotor speed. King and colleagues (1994) described that many (65%), but not all medial septal neurons exhibit a

linear increase in burst discharge rate as a function of speed. Thus, medial septal inputs may provide a key source of variation in relation to speed across the septotemporal axis. Such speed information may be transmitted to septal neurons via supramammillary, mid-line thalamic or brain stem afferents. Most importantly, there is considerable topographic variation in the organization of these ascending subcortical afferents both in their direct projections to the HPC as well as in their indirect inputs to medial septal neurons, which also project topographically throughout the septotemporal axis (Amaral and Kurz 1994).

Changes in theta and gamma indices are indicative of function

A growing body of evidence supports the idea that alterations of theta and/or gamma in rodent HPC can be linked to alterations in cognitive performance (see Montgomery et al, 2008; 2009; see also Jones and Wilson, 2005; Kay, 2005 and Martin, Beshel and Kay, 2007; Jutras et al., 2009; see also Ulanovsky and Moss, 2008). Similarly, a number of human studies have demonstrated a relationship between theta power and coherence within medial temporal lobe and other neocortical sites in relation to information processing (eg Fell et al., 2001; 2003; Sederberg et al., 2003; Raghavachari et al., 2006; Canolty et al., 2006; see Nyhus and Curran, 2010 for review). Our interest is focused on theta and/or gamma indices across the septotemporal axis as a means to examine the relationship between these neurophysiological indices, topographic

anatomy (eg, Dolorfo and Amaral, 1998) and functional differentiation across the long axis.

The present report emphasizes that a key component of theta power and theta coherence within predominantly the septal HPC is the locomotor speed of the animal. To our surprise, the relationship of locomotor speed to theta power varied substantially across the septotemporal axis. The present data point to speed contributing to as much as 40-60% in the variability of theta power at septal CA1 sites. Such findings contrast with reports linking theta to cognitive function and finding limited influence of locomotor speed on rodents performing spatial discrimination or memory task (eg, Montgomery et al. others). Further complicating matters, we observed both habituation (decreases in theta power as a function of speed) and septotemporal variation in the degree of habituation. Given the long history of attempts to link theta to function, and cautions in that regard (McFarland, 1975; Arnolds et al., 1984), the current findings highlight the need for systematic assessment of key variables including septotemporal position, laminar position and recent behavioral experience of animal. The observed findings however highlight the sheer dynamism of the theta signals and it would be of great interest to determine if the dominant relation of locomotor speed to theta power at septal CA1 sites could change depending upon behavioral context. Recent findings in our laboratory indicate that while navigation in novel spatial environments increases any number of theta indices, the speed to power relationship observed at septal sites is not altered. These findings however did not address one key possibility; could spatial navigation in a

memory-dependent task as compared to the present data set actually alter the variability in theta power related to speed at septal CA1 sites. Such a finding would figure prominently in theories of theta function (eg, Hasselmo et al., XXX; Lisman et al.,).

In summary, the theta LFP signal is far from a sinusoidal wave temporally gating the discharge of HPC neurons, but rather reflects the dynamic interaction of competing and cooperating inputs, which vary across the dendritic field of HPC and EC neurons. In this regard, systematic assessment of this signal could provide a unique spatial and temporal window into the dynamic flow of afferent input across the dendritic field of HPC and EC neurons. That signal offers a profoundly different spatial and temporal window into the neurophysiology of HPC and EC circuits as compared to the discharge of isolated units or ensembles of neurons (see Ohmed and Mehta, 2009 for review) or the BOLD signals provided by neuroimaging experiments (cite reference).

Chapter 3

Discussion

The present work demonstrates substantial septotemporal variation in the behavioral correlates of various spectral indices of theta within the hippocampal formation. The spatial behavioral correlate of locomotor speed decreased in influence from septal levels of HPC to more temporal levels, while the non-spatial correlate of number of exposures to the same maze increased in influence from septal to temporal levels of HPC. These two opposing septotemporal gradients complement behavioral work that has shown that the septal HPC processes spatial information, while the temporal HPC is involved in the processing of non-spatial emotional and motivational information.

Since there is a gradient of speed modulation along the septotemporal axis, it is likely that one or more of the topographically organized afferent systems are responsible for conveying the locomotor information to the septal HPC. The EC would appear to be well situated to provide such a graded speed input across the septotemporal axis of the HPC, since each segregate band in EC projects to septotemporally distinct domains of HPC. Also, the firing rates of pyramidal and stellate cells in the superficial layers of EC have been shown to be positively modulated by locomotor speed (Sargolini et al., 2006). If the EC were the source of the graded speed signal to the HPC, then we would expect to see differences in the speed modulation of theta power across the bands of the EC. Yet the current data suggests that the EC is not the source of the graded speed

signal to the HPC, since theta power was equally speed modulated in all regions of EC that we investigated.

A second topographically organized afferent system that could potentially be involved in the graded speed modulation across the septotemporal axis is the input from the medial septum. While it is unclear whether there is a septotemporal gradient in the density of input from MS, the septohippocampal cells display a topography within MS. So cells located posteriorly and medially project to septal levels of HPC, while MS cells located anteriorly and laterally project to temporal levels. Differences in the firing properties of these cells could result in the pattern of speed modulation observed along the septotemporal axis, although little information is available regarding the firing of MS cells in awake behaving animals. What little work that has been done has not considered the topographical location within MS of the cells being recorded.

A third potential candidate afferent comes from the supramammillary nucleus. The input from the supramammillary nucleus to the HPC decreases in density from septal to temporal levels (Vertes, 1992) and lesions of SUM disrupt the relationship between locomotor speed and CA1 pyramidal cell firing rate (Sharp and Koester, 2008). This latter point is highly suggestive that SUM plays a role in the speed modulation of theta power, but the laminar distribution of SUM terminals calls this into question. SUM afferents terminate in DG, CA2 and CA3a, but do not terminate in CA1. If the SUM input to HPC was responsible for the pattern of speed modulation observed in the current dataset, then the expectation would be that the density of input would be higher in CA1 than in DG

and show a septotemporal gradient in each region. While the septotemporal gradient is present, the laminar profile does not match.

An alternative means by which the SUM could influence HPC physiology is through its innervation of MS, thus providing an indirect influence. The SUM projects to both the HPC and MS, but the cells of origin may be from two non-overlapping populations within SUM (Vertes, 1988; Haglund et al., 1984). The fact that lesions of SUM result in a disruption of the relationship between speed and the firing rate of CA1 place cells, without a direct SUM projection to CA1, suggests that this indirect pathway may in fact play a role in the speed modulation of hippocampal physiology.

The decrease in theta power at more temporal levels of HPC with repeated exposures to the same maze within a given day is a clear example of a non-spatial manipulation that results in a graded response along the septotemporal axis. Of particular note, this graded response to a non-spatial manipulation is septotemporally opposite to the graded response of the influence of locomotor speed, which is clearly a spatially related variable. As the exact same maze was used for each of the recordings and no changes were made to the recording environment between recordings (ie, all proximal and distal cues remained the same), the theta power habituation likely arises from something internal to the animal. As Royer et al. (2010) suggested for temporal HPC, two possibilities are the emotional relevance and the goal-directedness or motivational state of the animal. This latter possibility seems unlikely. While it is difficult to ascertain the motivational state of a rat, a common method given the

simple locomotor task involved is to look at how fast the rats perform the task. Thus this method assumes that the faster a rat performs the task the greater the motivation and vice versa. Four of the six rats actually had faster mean trial speeds during the last recording session than during the first recording session. It can only be purely speculation as to whether a change in the emotional relevance of the recording situation is the cause of the habituation in theta power. The rats had been trained to run on the maze for months prior to the recordings, so they were well accustomed to the maze, the room and task. So while it may seem reasonable to suggest that with each successive exposure to the maze the emotional relevance of the setting diminished, that would assume that each day the experimental setting regained some emotional salience.

Importance of controlling for speed and habituation when designing experiments

The findings of the current work should inform future studies of many different types involving spectral indices in awake behaving rats. Many manipulations result in alterations in the animals overt behavior and those changes on their own will cause changes in spectral indices of theta. For example, systemic ketamine injections cause motor impairments in rats, with the end result typically being slower locomotor speeds. Without taking into consideration the slower speeds, the potentially erroneous conclusion could be drawn that a decrease in theta power was caused by the ketamine when it could just be a result of the slower speed of the animal.

The theta power habituation result should also be informative to the design of pharmacological studies. If the temporal profile of a pharmacological agent is being investigated through repeated recordings over time, then the fact that theta power habituates with repeated exposures to the same maze within a day must be taken into consideration. It could appear that a drug selectively decreases theta power at more temporal levels, but in fact the decrease could simply be the habituation that would be seen anyway. In fact, any study where animals are tested repeatedly on the same maze or tested a second time with some manipulation to the testing environment performed (eg, novel maze configuration), the temporal HPC theta power habituation needs to be taken into consideration. Theta power in the third quartile of CA1 is decreased even five minutes after an initial exposure to a familiar maze when rats are returned to the same maze ($A_1 \rightarrow A_2$). So a recording protocol where rats are returned to an altered maze for a second (or more) recording session ($A_1 \rightarrow A_2'$) should make a comparison to the analogous recording session from the habituation paradigm (compare A_2' to A_2 , instead of A_2' to A_1). Demonstrating that theta power at a third quartile CA1 site does not change from a baseline recording during the recording session on the altered maze (which is the second recording session of the day) may actually be demonstrating that the theta power habituation has been blocked by the environmental manipulation. There has been no change from the first recording, but theta power is increased over the level to be expected given a second recording on the same maze.

Future Directions

Based on the findings of the current work, several future lines of research would be warranted. One possibility would be to further investigate the source of the gradient in speed modulation along the septotemporal axis of the HPC. Since there is not one clear afferent that matches the septotemporal and transverse profile of the speed modulation it is likely that several afferent systems are involved. Manipulation of the potential afferent systems via lesion or pharmacological manipulation could provide information regarding the contribution a particular region makes to the speed modulation of theta in the HPC.

The two most likely candidate regions are the MS and supramammillary nucleus, as a majority of MS cells increase their bursting rate as a function of locomotor speed (King et al., 1998) and lesions of the supramammillary nucleus have been shown to decrease the speed modulation of CA1 place cell firing rates (Sharp and Koester, 2008). A complete lesion of the MS will abolish theta in the HPC and a selective lesion of just the cholinergic neurons of the MS will attenuate the amplitude of theta such that there would be little for locomotor speed to modulate. As a result, pharmacological manipulation with a cholinergic antagonist (eg, scopolamine) could decrease the contribution of cholinergic input from MS while still leaving theta fairly intact to be potentially modulated by locomotor speed. As little information regarding the role of the supramammillary nucleus on theta generation in the awake behaving rat is available, investigating

the effects of a supramammillary nucleus lesion or temporary inactivation on the speed modulation of theta, as well as on theta generation in general, would be informative.

In the case of the cholinergic manipulation, the analysis would simply require a comparison of the relationship between locomotor speed and theta power before and after the drug administration (ie, is there a change in the amount of theta power variability that locomotor speed explains?). A study involving the temporary inactivation of the supramammillary nucleus would involve the same design as the aforementioned cholinergic study, but the supramammillary nucleus lesion study would require a between groups design. The amount of theta power variability that is explained by locomotor speed in control animals would be compared to that in the lesion animals. The between groups design has the added complication that the two groups should have matching laminar placements, whereas the within subject pharmacological studies can identify changes in the speed versus theta power relationship within an electrode as a function of the pharmacological agent.

In addition to investigating the source of the speed modulation of theta in the HPC, another line of studies could look at the theta power habituation found at the more temporal levels of the septotemporal axis with repeated exposures to the same maze within a day. Considering the fact that the temporal HPC may be processing motivational and emotional information, manipulations of these two aspects may have a bearing on the habituation. Two potential ways to manipulate the motivational state of the animal are to systematically alter the

animals' weight through varying degrees of food restriction. A rat that has been food restricted to a lower percentage of its ad libitum weight should be more motivated to run for a food reward than a rat that has been food restricted less. The hypothesis would be that the more motivated rat would show less theta power habituation than the less motivated rat. The second potential way to manipulate the rats' motivational state is to change the food reward during one of the later recording sessions. One potential issue with this possibility is that the change in food is a form of novelty and the hippocampus is known to detect novelty.

A potentially more intriguing line of work involves investigating whether engaging the HPC in with some cognitive demand alters the influence of locomotor speed. Recently the suggestion has been made that speed is less influential when rats perform a cognitive task (Montgomery et al., 2009). This can easily be tested in several different ways. It is known that the HPC responds to novelty (Jeewajee et al., 2008), so a comparison of the influence of locomotor speed in a familiar environment versus a

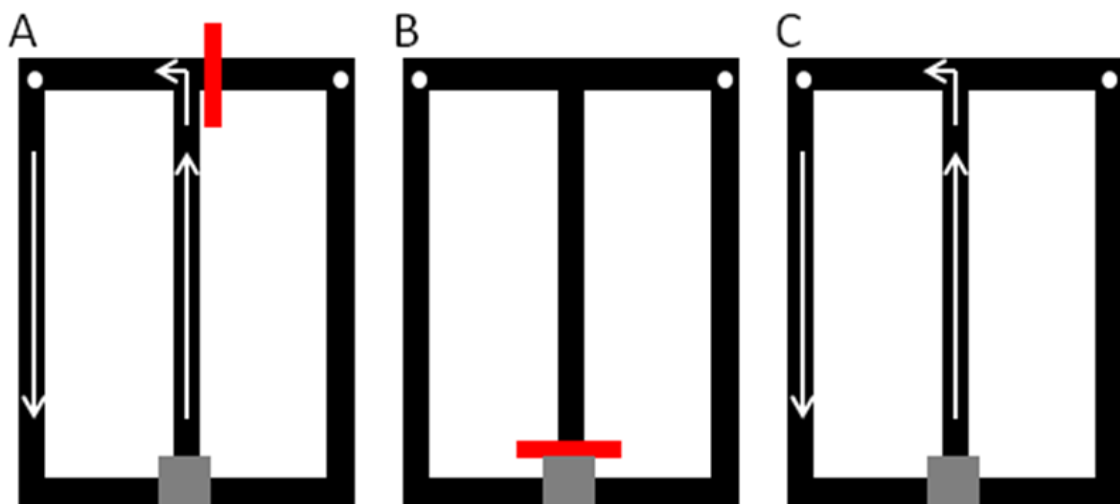


Figure 8. A) During the forced sample trial, the rat exits the start area (gray) and runs up the middle stem toward the choice point. A barrier is in place that forces the rat to make a turn to the left (trials will be presented randomly) where a food reward is found. The rat then runs back to the start area via the outside arm. B) The rat is blocked from exiting the start area for a variable delay. C) The rat runs up the middle stem and must make a turn matching the forced turn from the sample trial (in this case left). The rat receives a food reward and runs back to the start area via the outside arm. The speed modulation of theta power on the middle stem of C) can be compared to that on the return trip made via the outside arm. There is a clear cognitive component to the middle stem traversal, while no cognitive demands are put on the rat during the return trip.

novel environment could be made. In a similar manner, a memory task could be used to probe this issue. A delayed match (or non-match) to place task on a modified T-maze could be used (Figure 8). On the choice trial (Figure 8C), the rat has to make a decision while traversing the middle stem, but then returns to the start area via the outside arm with no cognitive demand being placed on it. The speed modulation of theta power on the middle stem could be compared to the return trip on the outside arm of the maze. The expectation based on the suggestion of Montgomery et al. (2009) would be that while in the novel environment or on the middle stem of the delayed match to place task locomotor speed would be less influential than in the familiar environment or on the outside arm during the delay task respectively. Based on the speed modulation and habituation data presented above it seems that a simple upward or downward shift of the linear best fit line for the relationship between locomotor speed and theta power would be more likely. Thus an overall change in theta power would be observed, but locomotor speed would still modulate theta power within each environment and task phase.

Conclusion

Both the speed modulation and the habituation of theta show how dynamic theta is over time, as well as the fact that theta can vary independently at different septotemporal levels. The present findings not only indicate that different behavioral variables influence indices of theta at different septotemporal levels beyond what has previously been shown, but they also necessitate that additional considerations need to be taken when designing and analyzing future experiments.

References

- Ahmed OJ, Mehta MR (2009) The hippocampal rate code: anatomy, physiology and theory. *Trends Neurosci* 32: 329-38.
- Alonso A, Garcia-Austt (1987) Neuronal sources of theta rhythm in the entorhinal cortex of the rat. I. Laminar Distribution of theta field potentials. *Exp Brain Res* 67: 493-501.
- Amaral DG, Kurz J (1985) An analysis of the origins of the cholinergic and noncholinergic septal projections to the hippocampal formation of the rat. *J Comp Neurol* 240: 37-59.
- Amaral DG, Witter, MP (1995) The three-dimensional organization of the hippocampal formation: a review of anatomical data. *Neuroscience* 31:371-391.
- Arnolds DE, Lopes da Silva RH, Boeijinga P, Kamp A, Aitink W (1984) Hippocampal EEG and motor activity in the cat: the role of eye movements and body acceleration. *Behav Brain Res* 12: 121-35.
- Axmacher N, Henseler MM, Jensen O, Weinreich I, Elger CE, Fell J (2010) Cross-frequency coupling supports multi-item working memory in the human hippocampus. *Proc Natl Acad Sci* 107: 3228-33.
- Bland BH (1986) Physiology and pharmacology of hippocampal formation theta rhythms. *Prog in Neurobiology* 26:1-54.
- Bland BH, Oddie SD (2001) Theta band oscillation and synchrony in the hippocampal formation and associated structures: the case for its role in sensorimotor integration. *Behav Brain Res* 127:119-36.
- Borhegyi Z, Varga V, Szilagyi N, Fado D, Freund TF (2004) Phase segregation of medial septal GABAergic neurons during hippocampal theta activity. *J Neurosci* 24:8470-9.
- Bouwman BM, van Lier H, Nitert HE, Drinkenburg WH, Coenen AM, van Rijn CM (2005) The relationship between hippocampal EEG theta activity and locomotor behavior in freely moving rats: effects of vigabatrin. *Brain Res Bull* 64: 505-9.
- Bragin A, Jando G, Nadasdy Z, Hetke J, Wise K, Buzsaki G (1995) Gamma (40-100 Hz) oscillation in the hippocampus of the behaving rat. *J Neurosci* 15:47-60.
- Brazhnik ES, Fox SE (1999) Action potentials and relations to the theta rhythm of medial septal neurons in vivo. *Exp Brain Res* 127: 244-58.

- Bullock TH, Buzsaki G, McClune MC (1990) Coherence of compound field potentials reveals discontinuities in the CA1-subiculum of the hippocampus of the freely-moving rat. *Neuroscience* 38:609-619.
- Buzsaki G (2002) Theta oscillations in the hippocampus. *Neuron* 33:325-340.
- Canolty RT, Edwards E, Dalal SS, Soltani M, Nagarajan SS, Kirsch HE, Berger MS, Barbaro NM, Knight RT (2006) High gamma power is phase-locked to theta oscillations in human neocortex. *Science* 313: 1626-8.
- Chrobak JJ, Amaral DG (2007) Entorhinal cortex of the monkey: VII. Intrinsic connections. *J Comp Neurol* 500: 612-33.
- Chrobak JJ, Buzsaki, G (1998) Gamma oscillations in the entorhinal cortex of the freely behaving rat. *J Neurosci* 18:388-398.
- Chrobak JJ, Buzsaki G (1994) Selective activation of deep layer (V-VI) retrohippocampal cortical neurons during hippocampal sharp waves in the behaving rat. *J Neurosci* 14:6160-70.
- Csicsvari J, Jamieson B, Wise KD, Buzsaki G (2003) Mechanisms of gamma oscillations of the behaving rat. *Neuron* 37:311-322.
- Dolorfo C, Amaral DG (1998a) Entorhinal cortex of the rat: Topographic organization of the cells of origin of the perforant path projections to the dentate gyrus. *J Comp Neurol* 398:25-48.
- Dolorfo CL, Amaral DG (1998b) Entorhinal cortex of the rat: organization of intrinsic connections. *J Comp Neurol* 398:49-82.
- Efron, B., & Tibshirani, R. J. (1993). An introduction to the bootstrap. New York: Chapman & Hall.
- Feder R, Ranck JB Jr (1973) Studies on single neurons in dorsal hippocampal formation and septum of unrestrained rats. II. Hippocampal slow waves and theta cell firing during bar pressing and other behaviors. *Exp Neurol* 41: 532-55.
- Fell J, Klaver P, Lehnertz K, Grunwald T, Schaller C, Elger CE, Fernandez G. (2001) Human memory formation is accompanied by rhinal-hippocampal coupling and decoupling. *Nat Neurosci.* Dec;4(12):1259-64.
- Freund TF, Antal M (1988) GABA-containing neurons in the septum control inhibitory interneurons in the hippocampus. *Nature* 336:170-173.
- Freund TF, Buzsaki G (1996) Interneurons of the hippocampus. *Hippocampus* 6: 347-470.

- Gage FH, Thompson RG (1980) Differential distribution of norepinephrine and serotonin along the dorsal-ventral axis of the hippocampal formation. *Brain Res Bull* 5: 771-3.
- Green JD, Arduini AA (1954) Hippocampal electrical activity in arousal. *J Neurophysiol* 17: 533-57.
- Haglund L, Swanson LW, Kohler C (1984) The projection of the supramammillary nucleus to the hippocampal formation: An immunohistochemical and anterograde transport study with the lectin PHA-L in the rat. *J Comp Neurol* 229: 171-185.
- Hajos N, Palhalmi J, Mann EO, Nemeth B, Paulsen O, Freund TF (2004) Spike timing of distinct types of GABAergic interneurons during hippocampal gamma oscillations in vitro. *J Neurosci* 24: 9127-37.
- Hangya B, Borhegyi Z, Szilagyi N, Freund TF, Varga V (2009) GABAergic neurons of the medial septum lead the hippocampal network during theta activity. *J Neurosci* 29: 8094-102.
- Hentschke H, Perkins MG, Perce RA, Banks MI (2007) Muscarinic blockade weakens interaction of gamma with theta rhythms in mouse hippocampus. *Eur J Neurosci* 26: 1642-56.
- Hyman JM, Zilli EA, Paley AM, Hasselmo ME (2005) Medial prefrontal cortex cells show dynamic modulation with the hippocampal theta rhythm dependent on behavior. *Hippocampus* 15: 739-49.
- Jeewajee A, Lever C, Burton S, O'Keefe J, Burgess N (2008) Environmental novelty is signaled by reduction of the hippocampal theta frequency. *Hippocampus* 18: 340-8.
- Jones MW, Wilson MA (2005) Theta rhythms coordinate hippocampal-prefrontal interactions in a spatial memory task. *PLoS Biol* 3: e402.
- Jung MW, Wiener SI, McNaughton BL (1994) Comparison of spatial firing characteristics of units in dorsal and ventral hippocampus of the rat. *J Neurosci* 14: 7347-56.
- Jutras MJ, Fries P, Buffalo EA (2009) Gamma-band synchronization in the macaque hippocampus and memory formation. *J Neurosci* 29: 12521-31.
- Kay LM (2005) Theta oscillations and sensorimotor performance. *Proc Natl Acad Sci* 102:3863-8.

- King C, Recce M, O'Keefe J (1998) The rhythmicity of cells of the medial septum/diagonal band of Broca in the awake freely moving rat: relationship with behavior and hippocampal theta. *Eur J Neurosci* 10: 464-77.
- Kjelstrup KB, Solstad T, Brun VH, Hafting T, Leutgeb S, Witter MP, Moser EI, Moser MB (2008) Finite scale of spatial representation in the hippocampus. *Science* 321: 140-3.
- Konopacki J, Bland BH, Colom LV, Oddie SD (1992) In vivo intracellular correlates of hippocampal formation theta-on and theta-off cells. *Brain Res* 586:247-55.
- Lorch RF Jr, Myers JL (1990) Regression analyses of repeated measures data in cognitive research. *J Exp Psychol Learn Mem Cogn* 16: 149-57.
- Lee MG, Chrobak JJ, Sik A, Wiley RG, Buzsaki G. (1994) Hippocampal theta activity following selective lesion of the septal cholinergic system. *Neuroscience* 62: 1033-47.
- Leung LS (1984) Pharmacology of theta phase shift in the hippocampal CA1 region of freely moving rats. *Electroencephalogr Clin Neurophysiol* 58: 457-66.
- Lisman JE, Idiart MA (1995) Storage of 7 +/- 2 sort-term memories in oscillatory subcycles. *Science* 267: 1512-5.
- Loy R, Koziell DA, Lindsey JD, Moore RY (1980) Noradrenergic innervations of the adult rat hippocampal formation. *J Comp Neurol* 189: 699-710.
- Manseau F, Goutagny R, Danik M, Williams S (2008) The hippocamposeptal pathway generates rhythmic firing of GABAergic neurons in the medial septum and diagonal bands: an investigation using a complete septohippocampal preparation in vitro. *J Neurosci* 28:4096-107.
- Martin C, Beshel J, Kay LM (2007) An olfacto-hippocampal network is dynamically involved in odor-discrimination learning. *J Neurophysiol* 98: 2196-205.
- Maurer AP, Cowen SL, Burke SN, Barnes CA, McNaughton BL (2005) Self-motion and the origin of differential spatial scaling along the septo-temporal axis of the hippocampus. *Hippocampus* 15: 841-52.
- McFarland WL, Teitelbaum H, Hedges EK (1975) Relationship between hippocampal theta activity and running speed in the rat. *J Comp Physiol Psychol* 88: 324-8.
- Montgomery SM, Sirota A, Buzsaki G (2008) Theta and gamma coordination of hippocampal networks during waking and rapid eye movement sleep. *J Neurosci* 28: 6731-41.

- Montgomery SM, Betancur MI, Buzsaki G (2009) Behavior-dependent coordination of multiple theta dipoles in the hippocampus. *J Neurosci* 29:1381-94.
- Nyhus E, Curran T (2010) Functional role of gamma and theta oscillations in episodic memory. *Neurosci Biobehav Rev* 34: 1023-35.
- O'Keefe J, Dostrovsky J (1971) The hippocampus as a spatial map. Preliminary evidence from unit activity in the freely-moving rat. *Brain Res* 34: 171-5.
- Oleskevich S, Descarries L (1990) Quantified distribution of serotonin innervations in adult rat hippocampus. *Neuroscience* 34: 19-33.
- Panula P, Pirvola U, Auvinen S, Airaksinen MS (1989) Histamine-immunoreactive nerve fibers in the rat brain. *Neuroscience* 28: 585-610.
- Petsche H, Stumpf C, Gogolak G (1962) The significance of the rabbit's septum as a relay station between the midbrain and the hippocampus. I. The control of the hippocampus arousal activity by the septum cells. *Electroencephalogr Clin Neurophysiol* 14: 202-11.
- Pikkarainen M, Ronkko S, Savander V, Insausti R, Pitkanen A (1999) Projections from the lateral, basal, and accessory basal nuclei of the amygdale to the hippocampal formation in rat. *J Comp Neurol* 403: 229-60.
- Raghavachari S, Lisman JE, Tully M, Madsen JR, Bromfield EB, Kahana MJ (2006) Theta oscillations in human cortex during a working-memory task:evidence for local generators. *J Neurophysiol* 95:1630-8.
- Rivas J, Gaztelu JM, Garcia-Austt E (1996) Changes in hippocampal cell discharge patterns and theta rhythm spectral properties as a function of walking velocity in the guinea pig. *Exp Brain Res* 108: 113-8.
- Roark RM, Escabi MA (1999). B-spline design of maximally flat and prolate spheroidal-type FIR filters. *IEEE Trans. on Signal Processing*, vol. 47, n. 3, pp. 701-716.
- Royer S, Sirota A, Patel J, Buzsaki G (2010) Distinct representations and theta dynamics in dorsal and ventral hippocampus. *J Neurosci* 30:1777-87.
- Sabolek HR, Penley SC, Hinman JR, Bunce JG, Markus EJ, Escabi M, Chrobak JJ (2009) Theta and gamma coherence along the septotemporal axis of the hippocampus. *J Neurophysiol* 101:1192-200.
- Sainsbury RS (1970) Hippocampal activity during natural behavior in the guinea pig. *Physiol Behav* 5: 317-24.

- Sargolini F, Fyhn M, Hafting T, McNaughton BL, Witter MP, Moser MB, Moser EI (2006) Conjunctive representation of position, direction, and velocity in entorhinal cortex. *Science* 312: 758-62.
- Sederberg PB, Kahana MJ, Howard MW, Donner EJ, Madsen JR (2003) Theta and gamma oscillations during encoding predict subsequent recall. *J Neurosci* 23: 10809-14.
- Sharp PE, Koester K (2008) Lesions of the mammillary body region alter hippocampal movement signals and theta frequency: implications for path integration models. *Hippocampus* 18: 862-78.
- Sharp PE, Turner-Williams S (2005) Movement-related correlates of single-cell activity in the medial mammillary nucleus of the rat during a pellet-chasing task. *J Neurophysiol* 94:1920-7.
- Shin J, Talnov A (2001) A single trial analysis of hippocampal theta frequency during nonsteady wheel running in rats. *Brain Res* 897: 217-21.
- Slawinska U, Kasicki S (1998) The frequency of rat's hippocampal theta rhythm is related to the speed of locomotion. *Brain Res* 796: 327-31.
- Steward O, Scoville SA (1976) Cells of origin of entorhinal cortical afferents to the hippocampus and fascia dentate of the rat. *J Comp Neurol* 169: 347-70.
- Swanson LW, Wyss JM, Cowan WM (1978) An autoradiographic study of the organization of intrahippocampal association pathways in the rat. *J Comp Neurol* 181:681-715.
- Swanson LW, Cowan WM (1977) An autoradiographic study of the organization of the efferent connections of the hippocampal formation in the rat. *J Comp Neurol* 172: 49-84.
- Teitelbaum H, McFarland WL (1971) Power spectral shifts in hippocampal EEG associated with conditioned locomotion in the rat. *Physiol Behav* 7: 545-9.
- Thompson CL, Pathak SD, Jeromin A, Ng LL, MacPherson CR, Mortrud MT, Cusick A, Riley ZL, Sunkin SM, Bernard A, Puchalski RB, Gage FH, Jones AR, Bajic VB, Hawrylycz MJ, Lein ES (2008) Genomic anatomy of the hippocampus. *Neuron* 60: 1010-21.
- Toth K, Borhegyi Z, Freund TF (1993) Postsynaptic targets of GABAergic hippocampal neurons in the medial septum-diagonal band of Broca complex. *J Neurosci* 13: 3712-24.
- Ulanovsky N, Moss CF (2007) Hippocampal cellular and network activity in freely

- moving echolocating bats. *Nat Neuroscience* 10:224-33.
- Vanderwolf CH (1969) Hippocampal electrical activity and voluntary movement in the rat. *Electroencephalogr Clin Neurophysiol* 26: 407-18.
- Vanderwolf CH (1971) Limbic-diencephalic mechanisms of voluntary movement. *Psychol Rev* 78: 83-113.
- Vertes RP (1988) Brainstem afferents to the basal forebrain in the rat. *Neuroscience* 24: 907-935.
- Vertes RP (1992) PHA-L analysis of projections from the supramammillary nucleus in the rat. *J Comp Neurol* 326: 595-622.
- Vertes RP, Kocsis B (1997) Brainstem-diencephalo-septohippocampal systems controlling the theta rhythm of the hippocampus. *Neuroscience* 81:893-926.
- Vertes RP, Hoover WB, Viana Di Prisco G (2004) Theta rhythm of the hippocampus: subcortical control and functional significance. *Behav Cogn Neurosci Rev* 3:173-200.
- Vertes RP, Hoover WB, Do Valle AC, Sherman A, Rodriguez JJ (2006) Efferent projections of reuniens and rhomboid nuclei of the thalamus in the rat. *J Comp Neurol* 499: 768-96.
- Vinogradova OS (1995) Expression, control, and probable functional significance of the neuronal theta-rhythm. *Prog Neurobiol* 45:523-583.
- Welch PD (1967) The use of fast fourier transform for the estimation of power spectra: a method based on time averaging over short, modified periodograms. *IEEE Trans Audio Electroacoust* 15:70-73.
- Whishaw IQ (1972) Hippocampal electroencephalographic activity in the Mongolian gerbil during natural behaviours and wheel running and in the rat during wheel running and conditioned immobility. *Can J Psychol* 26: 219-39.
- Whishaw IQ, Vanderwolf CH. (1973) Hippocampal EEG and behavior: changes in amplitude and frequency of RSA (theta rhythm) associated with spontaneous and learned movement patterns in rats and cats. *Behav Biol* 8:461-84.
- Wilson MA, McNaughton BL (1993) Dynamics of the hippocampal ensemble code for space. *Science* 261: 1055-8.
- Witter MP (2007) The perforant path: projections from the entorhinal cortex to the dentate gyrus. *Prog Brain Res* 163: 43-61.

- Wyble BP, Hyman JM, Rossi CA, Hasselmo ME. (2004) Analysis of theta power in hippocampal EEG during bar pressing and running behavior in rats during distinct behavioral contexts. *Hippocampus* 14:662-74.
- Ylinen A, Soltesz I, Bragin A, Penttonen M, Sik A, Buzsaki G (1995) Intracellular correlates of hippocampal theta rhythm in identified pyramidal cells, granule cells and basket cells. *Hippocampus* 5: 78-90.